DEUTSCHES ELEKTRONEN-SYNCHROTRON DESY

DESY SR 87-03
March 1987

DIFFRACTION EFFICIENCIES FOR THE HIGHER ORDERS OF A REFLECTION GRATING IN THE SOFT X-RAY REGION: COMPARISON BETWEEN THEORY AND EXPERIMENT

by

W. Jark

II. Institut f. Experimentalphysik, Universität Hamburg

M. Nevière

Laboratoire d'Optique Electromagnétique,

Faculté des Sciences, Marseille

ISSN 0723-7979

NOTKESTRASSE 85 · 2 HAMBURG 52

DESY SR 87-03
March 1987

ISSN 0723-7979

DIFFRACTION EFFICIENCIES FOR THE HIGHER ORDERS OF A REFLECTION GRATING IN THE SOFT X-RAY REGION: COMPARISON BETWEEN THEORY AND EXPERIMENT

W. Jark *

Universität Hamburg, II. Institut für Experimentalphysik, Luruper Chaussee 149, 2000 Hamburg 50, Fed. Rep. of Germany

M. Nevière

Laboratoire d'Optique Électromagnétique, Faculté des Sciences, Centre de St-Jérôme, 13397 Marseille Cedex 13, France

ABSTRACT

Diffraction efficiencies of a blazed grating measured in the soft x-ray region with photon energies between 60 eV and 925 eV are compared with calculations using the Differential Formalism of the exact electromagnetic theory. The parameters of the grating (gold coated with 1200 lines/mm and blaze angle 1.5°) are frequently used in soft X-ray monochromators. A quality check of this grating is made by investigating the total efficiency. Data for the -1., 0., +1., +2. and +3. order are presented, so that the suppression capability for higher harmonics can be derived. An application for the use of a blazed grating diffracting in 0. order is given.

* present address:

IBM Almaden Research Center, 650 Harry Road, San Jose, CA 95120-6099, USA

to be published in Appl. Opt.

INTRODUCTION

A major problem in the design of monochromators for the photon energy range 100 eV - 1000 eV (wavelength range 12.4 nm ≥ λ ≥ 1.24 nm) where the core levels of the important elements C, N and O are found is the lack of systematic experimental data about grating efficiencies. Only few measurements have been carried out in the cited energy range. While Lukirskii et al /1/ investigated systematically the diffraction efficiencies of ruled blazed grating, Haelbich et al /2/ reported extensive data for replica gratings for energies up to 230 eV (λ ≥ 5.5 nm) and Johnson /3/ compares different holographically recorded gratings for distinct energies of 283 eV (λ = 4.38 nm) and 1493 eV (λ = 0.83 nm).

No reliable data about the admixture of higher harmonics when illuminated with a continuous spectrum (for example synchrotron radiation) have been presented. Only the theoretical results by using the Differential Formalism /4/ of the exact electromagnetic theory were published for higher order efficiencies /5/. With this Differential Formalism a good agreement between the calculations for the 0. +1. and -1. order efficiencies and the investigations by Johnson /3/ was found for some examples /6/. Higher orders were not inspected in this study /6/.

We are presenting here the results of an investigation performed at a gold coated holographically blazed grating (blaze angle γ = 1.5°) with groove density 1200/mm. These parameters are most frequently chosen for instruments covering the above mentioned energy range. Calculations using the Differential Formalism will be compared to the measured data.

THE THEORY IN OUTLINE

The method which is used to compute grating efficiencies in the soft X-ray region is the Differential Formalism /4/. It is applicable to cylindrical bodies having generatrices parallel to the 0z axis of a Cartesian system 0xyz as shown in fig.1. Thus it cannot only handle classical gratings, but also gratings made with rods, phase gratings, or dielectric coated gratings, etc... Since we are interested here with classical gratings, we suppose that the directrix $\mathcal{D}$ of equation $y = g(x)$ is periodic in x with period d, and separates from free-space a medium of complex refractive index ν. The incident plane wave with wavelength $\lambda = 2\pi/|\vec{k}|$ impinges the grating under incidence θ.

Of the two principal cases of polarization (TE and TM), we will describe the formalism for the former. Thus the unknown function of the problem is the complex amplitude E(x,y) of the only non zero component of the electric field, that associated with the 0z axis. The main idea of the method is to find, for E(x,y), a propagation equation which is valid in the whole space in the sense of distributions or generalized functions, i.e. which includes the boundary conditions at the frontier of the two media. That partial derivative equation is then transformed into a set of coupled differential equations by Fourier Analysis, still valid in the whole space. Its integration is reduced to the shortest possible interval ($0 \le y \le a$, a : groove depth) due to the existence of analytical solutions for the field outside the modulated region. Inside the modulated region, the integration is done numerically on a computer. Let us now give some details on the different steps of the method.

Maxwell equations written in the whole space lead to the propagation equation:

$$\Delta E(x,y) + \alpha(x,y)\ E(x,y) = 0 \tag{1}$$

where $\alpha(x,y)$ is a known step function, periodic in x with period d, defined by:

$$\alpha(x,y) = k^2 \quad \text{if } y > g(x)\ ,$$
$$= k^2\nu^2 \quad \text{if } y < g(x)\ .$$

From the periodicity of the profile and the form of the incident field E^i, $E^i = \exp[ik(x \sin\theta - y\cos\theta)]$, it follows that E(x,y) is pseudo-periodic in x, which implies that $E(x,y)\exp(-ikx\sin\theta)$ is periodic and can be represented by its Fourier series. We thus obtain:

$$E(x,y) = \sum_{n=-\infty}^{+\infty} E_n(y)\ \exp(i\gamma_n x) \tag{2}$$

where

$$\gamma_n = k\sin\theta + nK, \quad K = 2\pi/d\ .$$

In a similar way, $\alpha(x,y)$ being periodic can be represented by:

$$\alpha(x,y) = \sum_{n=-\infty}^{+\infty} \alpha_n(y)\ \exp(inKx)\ , \tag{3}$$

where the Fourier coefficients $\alpha_n(y)$ can be derived from the knowledge of the groove shape ($y = g(x)$) and refractive index. Putting eqs. (2) and (3) in (1), we obtain the infinite set of differential equations:

$$\frac{d^2E_n}{dy^2} - \gamma_n^{\ 2}\ E_n(y) + \sum_{m=-\infty}^{+\infty} \alpha_{n-m}(y)\ E_m(y) = 0 \tag{4}$$

Outside of the modulated region, i.e. for $y > a$ or $y < 0$, the field can be represented by superpositions of plane waves, propagating or evanescent, called Rayleigh expansions:

if $y > a$:

$$E(x,y) = \exp[ik(x\sin\theta - y\cos\theta)] + \sum_{n=-\infty}^{+\infty} B_n \exp[i(\gamma_n x + \chi_n y)], \quad (5)$$

if $y < 0$:

$$E(x,y) = \sum_{n=-\infty}^{+\infty} T_n \exp[i(\gamma_n x + \chi'_n y)] , \quad (6)$$

where

$$\chi_n = \sqrt{k^2 - \gamma_n^2} \quad \text{if} \quad k^2 - \gamma_n^2 > 0$$

$$i\sqrt{\gamma_n^2 - k^2} \quad \text{if} \quad k^2 - \gamma_n^2 < 0$$

$$\chi'_n = \sqrt{k^2\nu^2 - \gamma_n^2} \quad \text{if} \quad k^2\nu^2 - \gamma_n^2 > 0$$

$$i\sqrt{\gamma_n^2 - k^2\nu^2} \quad \text{if} \quad k^2\nu^2 - \gamma_n^2 < 0 .$$

Thus outside the modulated region, the y-dependence of the Fourier coefficients $E_n(y)$ is already known. Only the Rayleigh coefficients B_n and T_n have to be determined. This is done by matching the numerical solution computed for $0 < y < a$ with the two Rayleigh expansions (5) and (6), the matching being done in such a way to ensure the continuity of both the function E(x,y) and of its y derivative. To this end, we first truncate the infinite set of to (2N + 1) equations (from n = -N to n = +N), where N is an integer which will have to be determined by numerical tests, but is typically equal to 5 or 6. We then consider (2N + 1) column vectors with (2N + 1) Elements $\tilde{E}_{np}(y)$ which are linearly independent and have the correct y dependence implied by equation (6) if $y < 0$. These elements are thus equal to $\exp(-i\chi'_n y)\,\delta_{np}$, where δ_{np} is the Kronecker symbol. From their values at y = -h and y = 0, where h is an integration step, a suitable integration algorithm can calculate $\tilde{E}_{np}(y)$ numerically for any value of y. The linear superposition:

$$E_n(y) = \sum_{p=-N}^{+N} T_p \tilde{E}_{np}(y) \quad (7)$$

thus satisfies (4) and (6).

It will be the solution of the problem if the unknown coefficients T_p are determined in such a way that the superposition (7) also satisfies (5). To that end, we write:

$$\sum_{p=-N}^{+N} T_p \tilde{E}_{np}(a+h) = \exp[-i\chi_n(a+h)]\delta_{no} + B_n \exp[i\chi_n(a+h)] , \quad (8)$$

$$\sum_{p=-N}^{+N} T_p \tilde{E}_{np}(a) = \exp[-i\chi_n a]\delta_{no} + B_n \exp[i\chi_n a] , \quad (9)$$

which ensures the continuity of both E(x,y) and its normal-derivative at the limit of the modulated region. From eqs. (8) and (9), a matrix inversion gives coefficients T_n, from which coefficients B_n are deduced through a matrix product.

The absolute efficiencies e_n in the n^{th} diffracted order are then given by:

$$e_n = B_n \bar{B}_n \frac{\chi_n}{\chi_o} .$$

with $\bar{B}_n$ the complex conjugated of B_n.

EXPERIMENTAL

The experiments were carried out with the UHV-Reflectometer described by Hogrefe et al /7/ at HASYLAB that uses the synchrotron radiation from the storage ring DORIS. Nearly all the precision requirements for accurate measurements given by Hunter /8/ are fulfilled in this instrument. It allows independent rotations and translations of the axes for the sample and the detector. The sample can thus be removed from the beam in order to detect the incident intensity without breaking the vacuum. This procedure can be repeated as often as necessary, hence the measured reflected intensity can be normalized easily and systematic errors due to detector sensitivity changes are very small in the derived data. Both axes can be rotated computercontrolled, which makes it possible to measure e.g. either the specularly reflected signal or the signal diffracted by a grating into a specified order dependent on the angle of incidence. After a calibration procedure for the angle encoders the rotations are performed so accurate that during an angle scan the reflected or diffracted signal will always optimally reach the entrance aperture of the detector. This aperture measures 1.25 mm in the plane of incidence and 3.2 mm in the perpendicular direction, while the halfwidth of the incident beam at the aperture 137 mm from the sample is 0.6 mm × 1.4 mm. In the detector the total photoelectron-yield at normal incidence from a stainless steel cathode coated with 15 nm Al_2O_3 is amplified in situ by a 20 stage open multiplier (Johnson MM1). The output is then measured outside the vacuum computerassisted with special current-to-voltage-converters /9/.

The monochromatized radiation in the soft x-ray region 50 eV to 1000 eV (24 nm $\geq \lambda \geq$ 1.25 nm) is supplied by the monochromator BUMBLE BEE, whose principles

and characteristic data are described in great detail elsewhere /10,11/. The higher order contributions in the detected signal can be reduced by proper choice of the scanning mode to below 1% in the mentioned energy range. A refocussing toroid behind the exit slit of the monochromator produces a highly collimated beam.

The investigated grating structure was holographically recorded into a resist on a quartz glass blank and afterwards transferred into the substrate by ion etching (manufacturer: ASTRON). It is a blazed profile with 1200 lines/mm and blaze angle $\gamma = 1.5°$. The gold coated grating was used for about 19 months in the FLIPPER monochromator /12/. In order to remove the carbon contamination layer the coating was stripped off and the substrate was recoated with 30 nm Au. The area ruled on the substrate (length 60 mm and width 40 mm) is a circle with diameter 52 mm, so that with beam dimensions at the sample of approximately 0.85 mm × 2.2 mm the efficiency can be measured for grazing angles of incidence as small as $\phi = 1.5°$.

The investigation was made with the grating in the classical orientation i.e. with the plane of incidence perpendicular to the groove edges and with unvignetted incident beam. The theoretical polarization of the radiation behind the exit slit of the monochromator is better than 87% /13/. The thus nearly linearly polarized electric field vector was oriented along the grooves, this situation, the TE case, is usually referred to as s-polarization. Systematic errors in the presented data are below 2%, hence the error bars are always smaller than the drawn symbols.

DISCUSSION

In order to show the relevance of our results first the quality of the grating is discussed. In our sign convention we call diffraction orders that lie between the incident and the specularly reflected beam positive orders or also inner orders. The factory measured maximum efficiency for the first inner order at wavelength $\lambda = 4.38$ nm was 10%, after the regeneration again an efficiency of 10% was measured at $\lambda = 4.5$ nm hence this grating is among the best in the category with groove density 1200/mm as can be seen from Johnson's comparative analysis /14/. The quality of this grating can also be shown more obvious in another way. By calculating the diffraction efficiencies for negligible blaze angle $\gamma \rightarrow 0^\circ$ the Differential Formalism for the efficiency calculation can be tested for consistency. In this case the total efficiency i.e. the sum of the efficiencies over all orders $e_t = \Sigma e_p$ should be identical to the Fresnel reflection coefficient of a simple mirror with the same coating. This test was successfully made in the original publication /4/ and is here repeated in fig. 2 for the parameters of the investigated grating. The modulation of this grating is small and as expected the calculations show only small differences between the total efficiencies and the reflection coefficients of a gold coated mirror. Hence the small deviations between the theoretical calculations and the experimental data which are also included in fig. 2 prove, that the grating is of high quality and will produce only small amounts of straylight.

For all calculations presented here with wavelengths λ shorter than 10 nm the optical constants were derived from the atomic scattering factors tabulated by Henke

et al /15/. For $\lambda = 20$ nm the optical constants were chosen from Hagemann et al /16/: $\varepsilon(\lambda = 20 \text{ nm}) = 0.714 + i\, 0.269$. This set of data is well suited for calculating the reflectivity of thin gold films in good agreement with the experiment /17/. The calculations were made for completely s-polarized light incident onto an ideal sawtooth profile. Interference effects caused by multiple reflections in the thin gold coating were not taken into account.

In figure 3 to 7 are presented the calculated and the measured efficiencies for the -1. to the +3. orders. Most of the wavelengths used for the investigation were chosen so that the contribution of higher orders can directly be derived. This can be done by comparing the efficiencies of e.g. the +3. order at $\lambda = 1.6$ nm and the +2. order at 2.5 nm with those for the +1. order of $\lambda = 5$ nm at the same angles of incidence.

The comparison between the calculated and the measured efficiencies for the 0. order in fig. 3 shows in all a good agreement for the 3 to 5 orders of magnitude that could be measured. Calculating the Fraunhofer diffraction caused by a shadowed facet, Lukirskii and Savinov /1/ derived the structure factor

$$S_q = \frac{\sin\left[(\pi b'/\lambda) \{\cos(\phi+\gamma) - \cos(\psi-\gamma)\}\right]}{(\pi b'/\lambda) \{\cos(\phi+\gamma) - \cos(\psi-\gamma)\}} \qquad (10)$$

where

$$b' = d\,[\cos\gamma - \sin\gamma\, \mathrm{ctg}(\phi+\gamma)] = d \cdot \frac{\sin\phi}{\sin(\phi+\gamma)}$$

is the illuminated length of the facet on a grating with the groove density 1/d. ϕ is the grazing angle of incidence, ψ the angle between the diffracted ray and the surface, γ the blaze angle and λ the wavelength of the incident radiation. One of the factors determining the efficiency is the square of this structure factor and indeed the minima in the curves in fig. 3 can very well be described by this factor with $\gamma = 1.5^\circ$. But there are some exceptions: for $\lambda = 10$ nm and $\phi \geq 20^\circ$ the minima do not longer coincide and larger deviations become obvious. Near $\lambda = 10$ nm the optical constants of gold and a glass substrate couple in such a way that multiple reflections in the thin film will modulate the reflectivity at steep angles of incidence where this reflectivity is usually small. This same effect is also to be expected where the efficiencies are very small, so the shape of the curves will here deviate from the calculations that do not take into account these multiple reflections /18/. The other exception is the first minimum in the curve for $\lambda = 1.6$ nm, this minimum is found for $\phi = 3.55^\circ$ while formula (10) predicts it at $\phi = 3.1^\circ$. Also this deviation can be explained. In most of the curves the slope changes suddenly between tangential incidence and the first minimum. At these noticeable points the first outer diffraction orders will lie just above the surface, so intensity is needed for these orders and must therefore be extracted from the other orders. Due to the coupling of the differential equations in the theoretical formulation of the diffraction problem the calculated efficiencies for the different orders are also not independent of each other, hence these slope changes also appear in the calculations. For $\lambda = 1.6$ nm this point lies at $\phi = 3.55^\circ$ which is in the observed minimum, thus the appearance of the -1. order shifts this minimum compared to formula (10). So in all the blaze angle of $\gamma = 1.5^\circ$ is very well confirmed.

The curve just discussed for $\lambda = 1.6$ nm gives additionally an impression for the purity of the incident monochromatic radiation from the monochromator BUMBLE BEE /11/. The efficiency reported for $\phi \geq 7^\circ$ (the curve element with very low slope) is mainly affected by straylight with longer wavelengths from the monochromator. The extrapolation of this tail to tangential incidence would determine the false signal in the incident beam to be of the order of 1%. After the end of this investigation absorption filters that suppress parts of the spectrum were installed behind the exit slit of the monochromator. By using these filters the agreement between theory and experiment could be significantly improved at this particular wavelength /19/.

The 0. diffraction order of a grating is normally of minor practical importance but the minima in fig. 3 characteristic for a blazed grating make obvious an interesting application. In monochromators that use independently rotatable axes for a premirror-grating combination as e.g. the Hunter /20/ monochromator and the BUMBLE BEE /10/ such a grating could be installed instead of the premirror for suppressing the higher orders. By using this grating in 0. order i.e. acting as a mirror we can adjust the configuration for a wavelength λ so that $\lambda/2$ is diffracted at the pre-grating just in its first efficiency minimum. The efficiency for $\lambda/2$ can then always be reduced to less than 1%, while it is at the same angles of incidence e.g. better than 20% for the nominal wavelengths $\lambda = 10$ nm and $\lambda = 20$ nm. For these two wavelengths this grating will thus reduce the second order contribution by about a factor of 100 with only moderate losses of the first order light.

The efficiencies for the first inner orders are shown for 5 wavelengths in fig. 4. Here differences are more obvious between the calculated and the measured efficiencies. The measured data are generally smaller than the calculated values, but the shapes of the experimental curves and the positions of the maxima are theoretically well reproduced. The minima, however, do not longer coincide but the spread of the data points does not allow to accurately determine the position of the experimental minima positions. Consequently the blaze angle that mainly determines the positions of these minima cannot be derived to a better degree than the anticipated 1.5°.

Contrary to the 0. orders abrupt slope changes caused by the appearance of the -1. order are no longer found in the experimental and theoretical curves for the other orders. The shapes of the curves for the -1. order efficiencies in fig. 5 are also very well reproduced by the theoretical calculations, but now the measured data are always higher than the theoretical expectations. While for the +1. orders the relative deviations between experiment and theory increase with decreasing wavelength, they decrease with decreasing wavelength for the -1. orders. This rather unsymmetrical intensity distribution among these two orders shows, that the actual directional character of this blazed grating is reduced compared to the predictions. This gives rise to the assumption, that the shape of the real grooves deviates from the ideal sawtooth profile. But on the other hand the blaze angle is confirmed very well and the total efficiency at $\lambda = 10$ nm is reduced only by a small amount compared to the calculations. So very small profile irregularities - mainly an imperfect groove edge - must be responsible for this reduced directional effect. This can also be one of the reasons for the deviations between theory and experiment that are obvious

for the higher diffraction (+2. and +3.) orders in fig. 6 and 7. With one exception the measured efficiency maxima for these orders are shifted compared to the calculations towards more grazing incidence. Only the experimental maximum for the +3. order of $\lambda = 10$ nm in fig. 7 is found at a steeper angle of incidence, but here all measured data are very small and as already explained for the 0. order multiple reflections in the thin gold coating can significantly affect the experimental data.

Consequently it is not possible to calculate reliable data for the higher order efficiencies of this blazed grating. However for grazing angles of incidence near the blaze maximum (i.e. the wave is reflected on the facet) and for larger angles the experimental data show better suppression capability for the higher orders than the theoretical predictions. Hence a theoretical optimization of the profile may give satisfying results for this situation, but our data do not allow to generalize this statement.

CONCLUSION

We can conclude, that it is possible to calculate in good agreement with the experiment the efficiency of a blazed grating in the 0. diffraction order. Normally this order is of minor practical importance but for a blazed grating an interesting application could be given. We could successfully calculate the shapes and the maxima positions of the efficiency curves for the first orders (+1. and -1.), but the measured absolute data differ from the theoretical calculations. We interpret this with a reduced directional character of the real blazed grating compared to the ideal sawtooth profile. Very small shape irregularities must be responsible for these deviations. The efficiency curves for the +2. and +3. orders could no longer be calculated satisfactorily, hence it seems not possible to calculate with reasonable reliability the contribution of higher orders for this real grating, that has been found to be of high quality. So the theoretically optimized data for the suppression of higher orders can significantly differ from data measured for a real grating and that even if the blaze angle is not deviating from the anticipated value.

One of us (W. J.) would like to thank C. Kunz for his support of the project and for many illuminating discussions as well as H. Hogrefe for his help during the early stages of the investigation. This work was supported by the Bundesministerium für Forschung und Technologie under contract No. 05 248 Ku and No. 05 305 AX B/5.

REFERENCES

/1/ A. P. Lukirskii and E. P. Savinov, "*Use of diffraction gratings and echelettes in the ultrasoft X-ray region*", Opt. Spectrosc. 14, 147 (1963)

A. P. Lukirskii, E. P. Savinov and Yu. P. Shepelev, "*Behaviour of gold and titanium coated echelettes in the 23.6 - 113 Å region*", Opt. Spectrosc. 15, 290 (1963)

/2/ R.-P. Haelbich, C. Kunz, D. Rudolph and G. Schmahl, "*Efficiency of holographic laminar gratings and ruled blazed gratings in the wavelength range 55 - 560 Å*", Nucl. Instr. and Meth. 152, 127 (1978)

/3/ R. L. Johnson, "*Theory, manufacture and performance of holographic X-ray gratings*" Ph. D. thesis, Imperial College, London 1975

/4/ M. Nevière, P. Vincent and R. Petit, "*Sur la théorie du réseau conducteur et ses applications a l'optique*", Nouv. Rev. Opt. 5, 65 (1974)

/5/ M. Nevière and J. Flamand, "*X-ray gratings: Influence of groove geometry and groove spacing*", Proc. VI. Int. Conf. on Vacuum Ultraviolet Radiation Physics, Charlottesville 1980, Extended Abstracts Vol III - 16

M. Nevière and J. Flamand, "*XUV grating contamination due to overlapping orders: A study through the electromagnetic theory*", Proc. of the VII. Int. Conf. on VUV Radiation Physics, Jerusalem 1983, Ed.: A. Weinreb and A. Ron, Annals of the Israel Physical Society Vol. 6, 45 (1983)

/6/ M. Nevière, "*Comparison between electromagnetic theory predictions and experimental results on X-ray gratings*", Proc. VI. Int. Conf. on Vacuum Ultraviolet Radiation Physics, Charlottesville 1980, Extended Abstracts Vol III - 15

/7/ H. Hogrefe, D. Giesenberg, R.-P. Haelbich and C. Kunz, "*A new VUV-reflectometer for UHV-applications*", Nucl. Instr. and Meth. 208, 415 (1983)

/8/ W.R. Hunter, "*On the cause of errors in reflectance vs. angle of incidence measurements and the design of reflectometers to eliminate the errors*", Appl. Opt. 6, 2140 (1967)

/9/ H. Vahldiek, "*Strom/Spannungs-Wandler verarbeitet geringe Signalströme*", Elektronik 10, 53 (1983)

/10/ W. Jark, R.-P. Haelbich, H. Hogrefe and C. Kunz, "*A new monochromator for the energy range $5\ eV \leq \hbar\omega \leq 1000\ eV$*", Nucl. Instr. and Meth. 208, 315 (1983)

/11/ W. Jark and C. Kunz, "*Output diagnostics of the grazing incidence plane grating monochromator Bumble Bee (15 - 1500 eV)*", Nucl. Instr. and Meth. A246, 320 (1986)

/12/ J. Barth, F. Gerken, C. Kunz and J. Schmidt-May, "*Grazing incidence monochromator Flipper*", Nucl. Instr. and Meth. 208, 307 (1983)

/13/ calculated for the monochromator entrance aperture with the program SPECTRA written by W. Graeff, HASYLAB

/14/ R. L. Johnson, "*Grazing incidence diffraction gratings*", Nucl. Instr. and Meth. 152, 117 (1978)

/15/ B. L. Henke, P. Lee, T. J. Tanaka, R. L. Shimabukuro and B. K. Fujikawa, "*Low-energy X-ray interaction coefficients: Photoabsorption, scattering, and reflection (E = 100 - 2000 eV, Z = 1 - 94)*", At. Dat. Nucl. Dat. Tables 27, 1 (1982)

/16/ H. J. Hagemann, W. Gudat and C. Kunz, "*Optical constants from the far infrared to the X-ray region: Mg, Al, Cu, Ag, Au, Bi, C, and Al_2O_3*", DESY Report SR-74/7 (1974), and J. Opt. Soc. Am. 65, 742 (1975)

/17/ W. Jark, "*Eigenschaften reflektierender optischer Komponenten und ihr Zusammenwirken in einem Monochromator für weiche Röntgenstrahlung (15 eV $\leq \hbar\omega \leq$ 1500 eV)*", thesis, Universität Hamburg 1985, DESY-HASYLAB Report 85-14, 1985

W. Jark, "*Enhancement of diffraction grating efficiencies in the soft X-ray region by a multilayer coating*", Opt. Commun. 60, 201 (1986)

/18/ For all other wavelengths this effect is less obvious as can e.g. be seen from reflectivities measured for a thin gold film and presented in /17/.

/19/ M. Krisch, Universität Hamburg, private communication 1986.

/20/ W. R. Hunter, R. T. Williams, J. C. Rife, J. P. Kirkland and M. N. Kabler, "*A grating/crystal monochromator for the spectral range 5 eV - 5 keV*", Nucl. Instr. and Meth. 195, 141 (1982)

FIGURE CAPTIONS

Fig. 1. Illustration of the parameters which are used for calculating the grating efficiencies.

Fig. 2. Total efficiency of a blazed grating coated with gold (1200/mm, $\gamma=1.5°$) dependent on the angle of grazing incidence for $\lambda=10$ nm: Comparison of the measured data (dots) with the calculations (open squares) and with the reflectivity calculated for an ideal gold mirror (solid line).

Fig. 3. Efficiency of a blazed grating coated with gold (1200/mm, $\gamma=1.5°$) dependent on the angle of grazing incidence for different wavelengths: Comparison of the measured data (dots) with the calculations (solid line) for the 0. order.

Fig. 4. same as fig. 3. but now for the +1. order.

Fig. 5. same as fig. 3. but now for the -1. order.

Fig. 6. same as fig. 3. but now for the +2. order.

Fig. 7. same as fig. 3. but now for the +3. order.

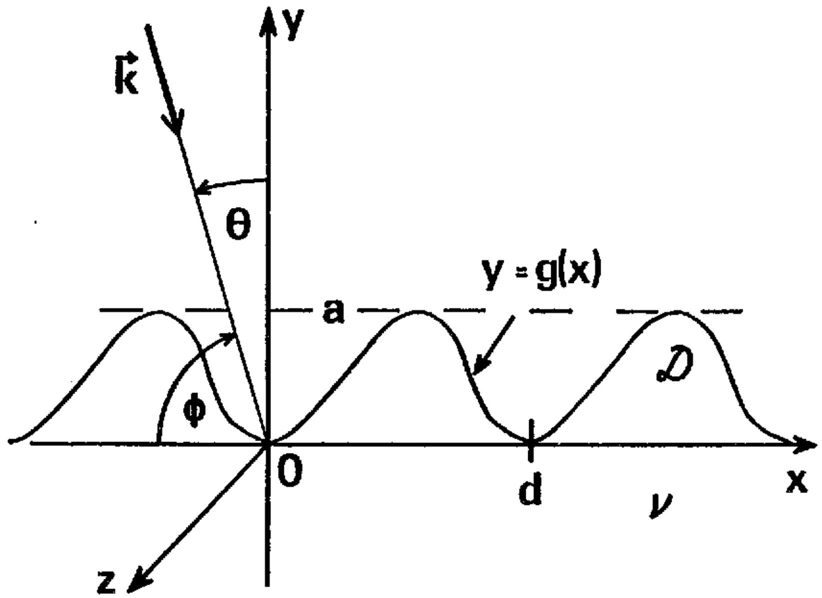

Fig. 1.

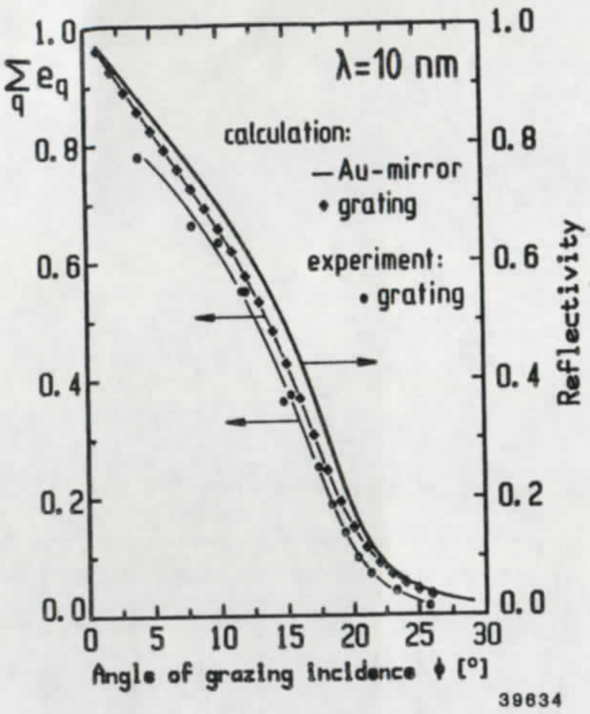
λ=10 nm
calculation:
—Au-mirror
• grating
experiment:
• grating
Reflectivity
Angle of grazing incidence ϕ [°]
39634

Fig. 2.

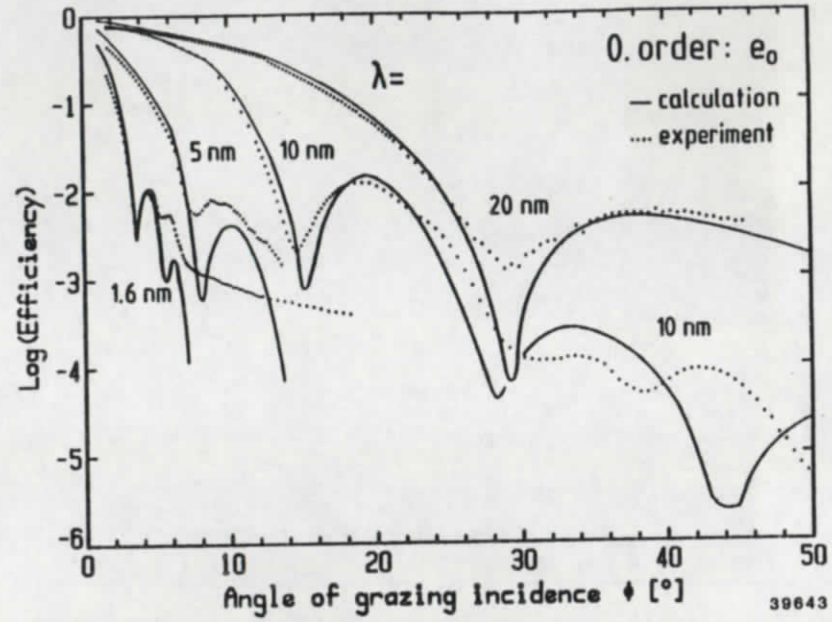
0. order: e₀
λ=
— calculation
.... experiment
5 nm
10 nm
20 nm
1.6 nm
10 nm
Log (Efficiency)
Angle of grazing incidence ϕ [°]
39643

Fig. 3.

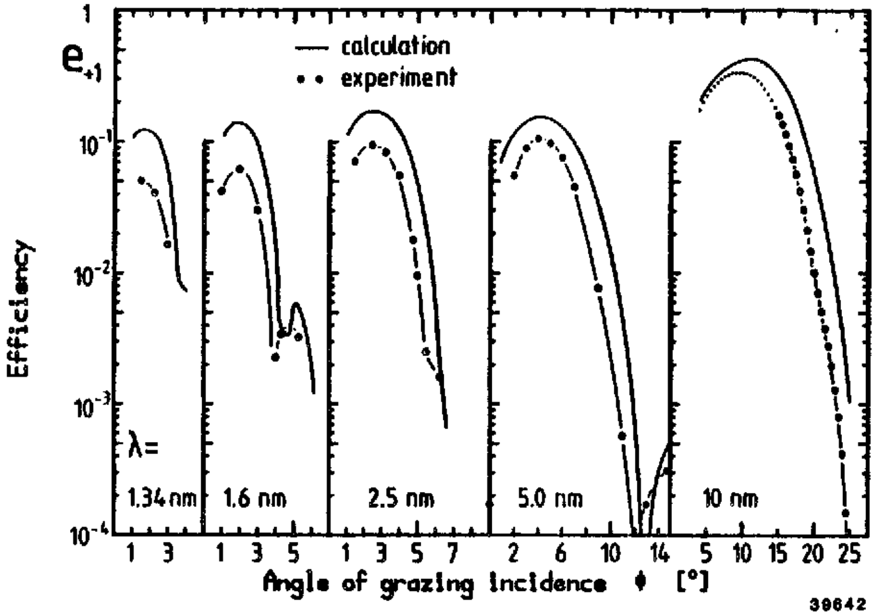

e+1
— calculation
• • experiment
Efficiency
1
10^-1
10^-2
10^-3
10^-4
λ=
1.34 nm
1.6 nm
2.5 nm
5.0 nm
10 nm
Angle of grazing incidence ϕ [°]
39642

Fig. 4.

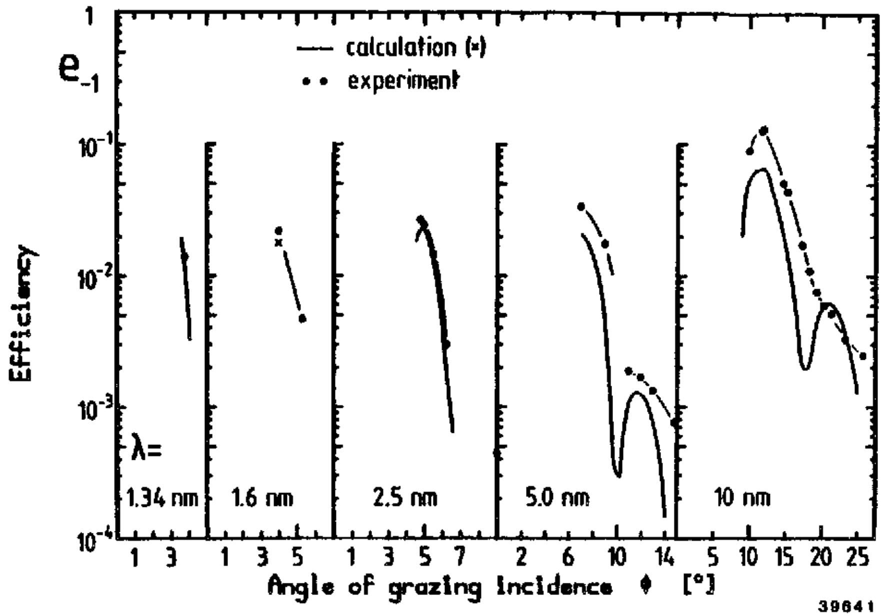

e-1
— calculation (×)
• • experiment
Efficiency
1
10^-1
10^-2
10^-3
10^-4
λ=
1.34 nm
1.6 nm
2.5 nm
5.0 nm
10 nm
Angle of grazing incidence ϕ [°]
39641

Fig. 5.

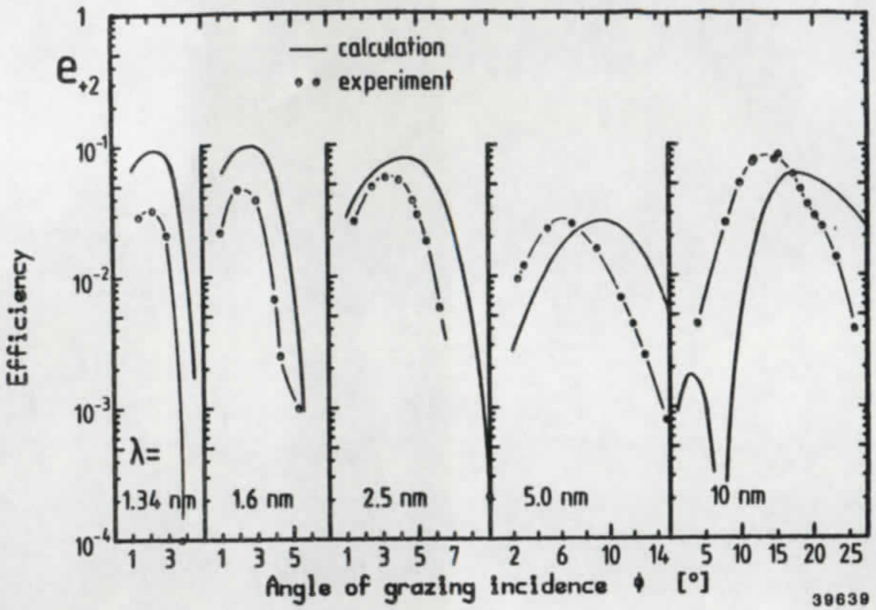

e+2
— calculation
• • experiment
Efficiency
1
10⁻¹
10⁻²
10⁻³
10⁻⁴
λ=
1.34 nm
1.6 nm
2.5 nm
5.0 nm
10 nm
1 3
1 3 5
1 3 5 7
2 6 10 14
5 10 15 20 25
Angle of grazing incidence ϕ [°]
39639

Fig. 6.

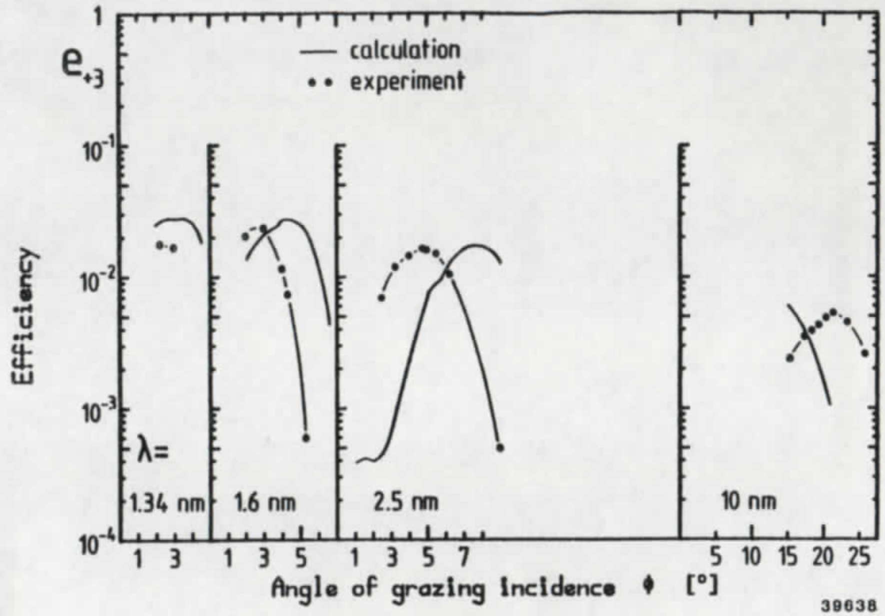

e+3
— calculation
• • experiment
Efficiency
1
10⁻¹
10⁻²
10⁻³
10⁻⁴
λ=
1.34 nm
1.6 nm
2.5 nm
10 nm
1 3
1 3 5
1 3 5 7
5 10 15 20 25
Angle of grazing incidence ϕ [°]
39638

Fig. 7.